THE PENNSYLVANIA STATE UNIVERSITY
SCHREYER HONORS COLLEGE

DEPARTMENT OF BIOLOGY

ROLE OF RON RECEPTOR TYROSINE KINASE IN ATHEROSCLEROTIC PLAQUE COMPOSITION

STACI HENRY
SPRING 2014

A thesis
submitted in partial fulfillment
of the requirements
for a baccalaureate degree in Biology
with honors in Biology

Reviewed and approved* by the following:

Pamela Hankey
Professor of Immunology
Thesis Supervisor

Bernhard Lüscher
Professor of Biology, Biochemistry and Molecular Biology
Honors Adviser

* Signatures are on file in the Schreyer Honors College.

ABSTRACT

Atherosclerosis is a chronic inflammatory disease the progression of which is mediated, in large part, by the balance of macrophages within the lesions. The progression of atherosclerosis is associated with an increase in infiltrating inflammatory macrophages (also called M1 macrophages) and a decrease in tissue-resident macrophages linked to healing and cell clearance (also called M2 macrophages). Ron is a receptor tyrosine kinase expressed on tissue-resident macrophages. *In vitro* and *in vivo*, Ron promotes the development of macrophages linked to wound repair and apoptotic cell clearance and inhibits the activation of inflammatory macrophages. Therefore, we hypothesized that Ron would play a protective role in the progression of atherosclerosis. In order to test this hypothesis, we examined the composition of atherosclerotic plaques formed in the aortic roots of eighteen-week-old mice in the presence and absence of Ron. We examined the deposition of collagen, the percentage of apoptotic cells, and the extent of necrosis using trichrome collagen staining and TUNEL assay. The results showed a significantly greater percentage of apoptotic cells present in plaques of mice in the presence of Ron, associated with a trend towards decreased necrosis in these plaques. However, we did not observe a significant difference in the amount of collagen deposition in the plaques from wild-type and Ron knockout animals. These data suggest that Ron may play a protective role in the progression of lesion formation, but may not protect against lesion rupture caused by decreased collagen in the fibrous cap.

TABLE OF CONTENTS

LIST OF FIGURES

LIST OF TABLES

ACKNOWLEDGEMENTS

This undergraduate honors thesis was completed in the lab of Dr. Pamela Hankey. I would like to thank Dr. Hankey for her help and guidance over the past two and a half years while in her research lab. I additionally want to thank Shan Yu and Joselyn Allen for all of their teaching and guidance during our time in the lab. I would also like to thank my honors advisor and thesis reader Dr. Bernhard Lüscher. Lastly, I would like to thank my father Vincent Henry and my sister Kristi Henry for their support throughout my undergraduate studies as well as my mother Diane Henry whose memory gives me the strength to continue to strive for excellence in all I do.

Chapter 1 : Introduction

Atherosclerosis

Cardiovascular disease, including coronary artery disease and cerebrovascular disease, is a major cause of mortality facing the world today[2]. Throughout the past few decades, our understanding of atherosclerosis as a disease has changed dramatically. Prior to these advances it was thought that atherosclerosis was a passive disease affecting lipid storage[2]. Today, atherosclerosis is characterized as a chronic inflammatory condition in which fatty streaks and plaque lesions form in the subendothelial portion of the blood vessels[3]. When the fatty lesions continue to advance they form thick fibrous caps and the interior begins to form necrotic tissue[1,25,26]. With continued progression of this necrotic area, there is an increased risk of rupture of these plaques, which can cause hemorrhaging and death[1,25]. While there is much research regarding various aspects of this chronic disease, there is a distinct lack of advancement toward therapies able to target the problems[1].

Atherosclerosis progresses in stages beginning with thickening of the intima infiltration of macrophage foam cells at the luminal surface[1,27]. As the lesions progress they form a necrotic core collecting cell debris along with a developing fibrous cap surrounding the area[1,25]. This cap becomes visually distinct as the lesion advances and starts to thin causing greater danger that the plaque will rupture[1,25]. It has been shown that, in these necrotic cores with thinning fibrous caps are many macrophages and T cells[1,28]. The macrophages in these advanced lesions play a central role in the development of atherosclerosis.

The connection between inflammation and atherosclerosis was a critical change in its study both in the way we look at risk factors as well as mechanisms and future treatments[3].

Inflammation participates in each stage of plaque progression[3]. Normal endothelium will not bind well with blood leukocytes however, in an early stage fatty streak when the endothelium starts to become inflamed it will express adhesion molecules[3]. As the lesion grows, T cells will join macrophages present in the forming lesion[3]. This can then promote induction of enzymes which function to degrade collagen found in the plaque as it responds to the inflammation[3]. In more advanced lesions, inhibition of collagen synthesis can take place, weakening the fibrous cap, due to the presence of inflammatory mediators[3]. This is supported by studies showing that patients diagnosed with chronic inflammatory diseases have a significantly higher risk of developing cardiovascular disease[2].

There is increasing evidence demonstrating a connection between inflammation and other health conditions that are widely considered triggers for such events[3]. These include diabetes, hypertension, and obesity[3]. Of much interest is the increasing evidence that inflammation could participate in hypertension, which would link it to atherosclerosis by way of pathophysiology[3]. While the composition of these fatty plaques is understood on a general level, but a more in depth look could aid in development of therapeutic techniques in the future. It is known that these plaques contain apoptotic cells, necrotic regions, cell debris, and cholesterol crystals[3]. Also present in both fatty streaks and established lesions are macrophages[5]. A better understanding of the role of macrophages in atherosclerosis may help to develop novel therapeutic techniques[5].

Macrophages

Macrophages are known to play a role in innate and adaptive immunity and are present throughout the body[5]. They are key players in metabolic inflammation and as such, play an important role in the progression of atherosclerosis[6,19]. Studies show that there are two extremes, or types, of macrophages[19]. This includes classically activated macrophages, often termed M1, at

one end of the spectrum and alternatively activated macrophages, termed M2, at the other[19]. The M1 type macrophages promote proinflammatory processes[5,29]. The M2 type, conversely, promote repair and resolution[5,29]. The presence of these types of macrophages in atherosclerotic lesions is of much interest in the field in recent years[5].

There has been a lot of research characterizing how changes in macrophage gene expression may affect the concentration of M1 or M2 macrophages present in atherosclerosis. Recent studies have shown arginase 1 (Arg 1) is a marker for M2 macrophages[19,21]. Arg 1 hydrolyzes L-arginine into urea which leads to the formation of polyamines as well as L-proline[19,21]. As the M2 macrophages are categorized in repair and resolution, so are the polyamines and L-proline[19,21]. Inflammatory M1 macrophages, on the other hand, express inducible nitric oxide synthase (iNOS) which competes for L-arginine to produce nitric oxide which is cytotoxic. Together these changes in the metabolism of L-arginine can affect the progression of atherosclerosis[21].

Arg 1 expression is induced in M2 macrophages in a Stat6-dependent manner by the Th2 cytokines, IL-4 and IL-13. However, recent studies have shown that Arg 1 expression is promoted through a Stat6-independent mechanism by the receptor tyrosine kinase, Ron[22]. In primary macrophages treated with macrophage stimulating protein, the ligand for Ron, MAPK is activated enhancing binding of AP-1 to the Arg 1 promotor[22]. Tumor-associated macrophages (TAMs) exhibit an M2 phenotype and promote tumor growth. In mice deficient of the Ron gene, the expression of Arg 1 is significantly reduced in tumor-associated macrophages, associated with decreased tumor growth[22]. This relationship between the Ron receptor and M2 macrophage activation, as measured by Arg 1 expression, suggests that Ron might also regulate the progression of atherosclerosis.

Ron Receptor Tyrosine Kinase

Ron is a receptor tyrosine kinase, and its ligand is macrophage-stimulating protein (MSP)[20]. MSP is primarily produced in the liver and circulates in an inactive form. Upon entering inflamed tissues, MSP becomes proteolytically cleaved and activated. Ron is a member of the MET gene family and has been shown to be involved in the regulation of immune responses by regulating macrophage activation[20]. In the immune system, Ron expressed in certain types of tissue-resident macrophages including Kupffer cells in the liver, mesangial cells in the kidney, microglia in the brain, marginal zone macrophages in the spleen, and resident peritoneal macrophages[23]. The specificity of its expression within the immune system suggests that it is tightly regulated within this population of cells[23].

Several studies have shown that Ron expression is crucial in limiting inflammatory responses[23]. Ron knockout mice are more susceptible to septic shock and acetaminophen-induced liver damage, associated with increased iNOS expression and increased pro-inflammatory cytokine production. Changes in the balance of M1 and M2 macrophages in the presence and absence of Ron may account for the differences in susceptibility to inflammatory disease[23]. A better understanding of this connection and how it relates to chronic inflammatory diseases, such as atherosclerosis, will likely provide novel techniques to identify and treat such problems.

Hypothesis

Based on its ability to inhibit M1 macrophage activation and promote an M2 phenotype, we hypothesized that the receptor tyrosine kinase Ron plays a protective role in the progression of atherosclerosis. The focus of the research was to study the possible similarities and differences in the composition of the atherosclerotic plaques between mice in the presence and absence of Ron.

The approach was to determine whether the composition of atherosclerotic plaques found in the aortic roots in ApoE knockout mice, which are predisposed to form atherosclerotic lesions on a high cholesterol diet, were changed based on the presence or absence of the receptor tyrosine kinase Ron.

Specifically, we hypothesized that a smaller percentage of the plaque area would be stained for collagen presence in the mice that lacked the Ron receptor. We hypothesized that there would be an increase in apoptotic cells present in the atherosclerotic plaques of the mice lacking the Ron receptor gene. Finally, we hypothesized that the necrotic core area would be greater in those mice lacking Ron.

Chapter 2 : Materials and Methods

Mouse Models

Two genotypes of mice were used in the research. Apolipoprotein E knock out ($ApoE^{-/-}$) mice on the C57BL/6 background were purchased from Jackson Laboratory (Bar Harbor, ME). The $ApoE^{-/-}$ mice are predisposed to form atherosclerotic lesions[15]. The other was a double gene knock out (DKO) of the ApoE ($ApoE^{-/-}$) gene and receptor tyrosine kinase Ron ($Ron^{-/-}$). To obtain the DKO genotype, $ApoE^{-/-}$ and $Ron^{-/-}$ mice were intercrossed. The Ron-/- mice were also on the C57BL/6 background. A polymerase chain reaction confirmed the DKO genotype. All of the mice were maintained and bred at the Pennsylvania State University animal facility following the protocol approved by the Institutional Animal Care and Use Committee (IUCAC).

Mice were fed a high cholesterol diet composed of 60% calories from fat plus 1.25% cholesterol (BioServ 6334) after being weaned at 5 weeks of age. The first 5 weeks all mice were fed a normal chow diet. All mice were sacrificed per IUCAC protocols at 18 weeks, so they were on the high cholesterol diet for a total of 13 weeks. The high cholesterol diet provided an accelerated model of metabolic disorder in order to study atherosclerotic progression in the mice. Both the single and double knockout mice were treated and analyzed equally throughout the experiments.

Aortic Root Samples

At 18 weeks, mice were sacrificed by carbon dioxide inhalation following IUCAC protocols. The hearts were isolated and snap frozen in optimal cutting temperature (OCT) media.

The isolated hearts were stored at a temperature of -80°C. The frozen samples were sectioned to expose and then collect 7µm thick sections form the aortic root area of the heart. The aortic root sections were prepared using the Shandon Cryostat, with a sample thickness of 7µm. This method was used as it kept the heart samples frozen and intact to allow for complete sections of the area in question. The aortic root slices were placed on glass slides and completed sections were stored at -80°C until the staining and analysis was to be completed

Trichrome Collagen Staining

The samples were sent for trichrome collagen staining to the Animal Diagnostic Laboratory at the Pennsylvania State University. The stained samples were then imaged under a microscope and the presence of collagen and necrotic area in the plaques were measured using Image J software as described below in the analysis techniques section.

TUNEL Assay

The TUNEL assay, terminal deoxynucleotidyl transferase end labeling, is used to label DNA strand breaks to identify cells that have begun to undergo apoptosis[17]. The TUNEL reaction labels the DNA strand breaks by a polymerization of labeled nucleotides to free 3'-OH ends[17]. The stained slides were analyzed using fluorescence microscopy to detect the apoptotic cells, tagged with green fluorescence protein (GFP). The samples were also stained with DAPI, which labeled the nuclei of the cells present in the section.

The assay procedure for cryopreserved sections involved multiple steps including fixation, permeablization, labeling the reaction with the TUNEL reaction mixture, and finally analysis of the samples using fluorescence microscopy. The *In Situ* Cell Death Detection Kit,

TMR Red, Version 11 was used for the assay. First, the tissue samples were fixed using the fixation solution for a total of 20 minutes at +15-25°C. Then, the samples were washed with PBS for 30 minutes. Next, the slides were placed in permeablization solution for 2 minutes completed on ice to be kept between +2°C and +8°C.

The TUNEL reaction mixture was prepared and kept on ice until use. Two negative controls and a positive control were included. The two negative controls had 2 samples incubated each in 50µl of label solution. No TUNEL reaction mixture was used on the negative controls. The positive control used a sample which was incubated in recombinant DNase I for 10 minutes between +15°C and +25°C. This was done to induce DNA strand breaks before the labeling procedure for the positive control.

The labeling procedure was then conducted for each sample. First, each slide was rinsed twice with PBS and the area around the sample was dried. Next, 50µl of the TUNEL reaction mixture was placed on each sample, excluding the negative control sample. The samples were covered with a coverslip for the following incubation. The slides were then incubated for 60 minutes at +37°C in the dark. After 60 minutes, the slides were rinsed 3 times with PBS. At this time the staining procedure was completed and the samples were then viewed and imaged by fluorescence microscopy.

Analysis Techniques

The analysis of the sample images for both the collagen staining and the TUNEL assay were done using Image J software. To begin with the trichrome collagen stain samples, the total plaque area on each image was isolated and the isolated plaque image was then used in the Image J analysis in order to measure collagen stained area, the total plaque area, and the necrotic area. Each image was taken as a 14.16in.X10.67in (1360X1040 pixels) image at 50x magnification.

For each sample the isolated plaque image, still 1360X1040 pixels and 14.16in.X10.67in., was opened in Image J and first converted to a grayscale 8-bit image (Image → Type → 8-bit). Next, the measurements were set (Set measurements → check "area" and "limit to threshold"). The scale was set to 96.012 pixels/inch. This measurement was used because we were not able to image the samples with a scale bar on the image and this would accurately measure the area since all pictures were taken with the same pixel dimensions and at the same magnification. Note that these measurements were used to look at the average percent of the total area the collagen and later necrotic area composed.

This threshold was adjusted to highlight all of the collagen stained area for measurement (Image → Adjust → Threshold) and the top and bottom threshold slide bars were set to 0 and 150, respectively. The collagen area measurement was then taken (Analyze → Measure) and the resulting area measurement was recorded (in inches^2, note this is the area based on its size in the image). Then, the threshold highlighted area was adjusted where the top and bottom slide bars were set to 0 and 248, respectively to cover the total plaque area. The total plaque area was measured (Analyze → Measure) and recorded. Next, the image colors were inverted to allow for threshold measurement of the necrotic area (Edit → Invert). As before, the threshold was adjusted to measure the necrotic area with the top and bottom slide bars set to 145 and 249 respectively. The necrotic plaque area was measured (Analyze → Measure) and recorded. The percent collagen area of the plaque was calculated [(collagen area/total plaque area)*100] and the percent necrotic area was calculated [(necrotic area/total plaque area)*100] and both were recorded. These steps were repeated for each collagen staining sample.

Image J was also used to complete the cell counts for the GFP and DAPI stained cells in the plaque area samples of the TUNEL assay. Before each sample image could be analyzed in Image J, the color was inverted (to show the stained areas on a lighter background) and each image was converted to black and white so the images could be analyzed with the software.

Then, each image was opened in Image J and the image type was converted into 8-bit (Image → Type → 8-bit). Next, the image threshold was set to highlight the stained areas (Process → Binary → Make Binary). The area of the plaque was selected for analysis and the particles were counted (Analyze → Analyze Particles). The cell count was completed for each GFP and DAPI sample image and recorded and the percent of apoptotic cells was calculated [(GFP cell count / DAPI cell count)*100] and recorded.

The necrotic area and total plaque area were also analyzed on the TUNEL images using Inage J. Each image was taken as a 14.16in.X10.67in (1360X1040 pixels) image at 50x magnification. Each image was opened and first set to 8-bit and then to RGB color (Image → Type → 8-bit / Image → Type → RGB color). The GFP and DAPI image for the specified sample were then merged to a single combined composite image, maintaining the 1360X1040 pixel size (Make composite → Merge channels). The total plaque area was then selected and measured (Analyze → Measure) in pixels and recorded. Next, the necrotic area (area lacking both stains) was selected and measured (Analyze → Measure) in pixels and recorded. The percent necrotic area was calculated [(necrotic area/total plaque area)*100] and recorded.

Chapter 3 : Results

In order to test the hypothesis, we analyzed the percentage of collagen deposition and the percentage of necrotic area within the plaque in the aortic roots of mice in the presence and absence of Ron using trichrome collagen staining. Aortic root sections were also analyzed using TUNEL assay to quantify the percentage of apoptotic cells in the plaques as well as the amount of necrosis. All complete data tables referred to in the results can be viewed in the Appendix.

Trichrome Collagen Staining

The aortic roots stained for collagen presence were imaged under a microscope at 50x magnification to observe the plaque area and specifically to allow us to analyze the collagen deposition and the visible necrotic core. All sample pictures were taken as a 14.16in.X10.67in. image containing 1360X1040 pixels, which was crucial to enable measurements of the areas as we were unable to image the samples with a scale bar. This uniform imaging allowed us to measure the area in $in.^2$ of the image since there was known to be 96.012 pixels per inch. All areas were measured using Image J software on images taken at the same magnification to ensure standard measurements using these parameters. In Figure 1 you can see examples of aortic root samples with the trichrome collagen stain for both the $ApoE^{-/-}$ and the $ApoE^{-/-}/Ron^{-/-}$ (DKO) genotypes. The images labeled (A) and (C) are the full stained sample image at 50x magnification (not the picture size has been reduced to fit on the page) and (B) and (D) are the isolation of the plaque visible in the aortic root used for Image J analysis of total area, collagen area, and necrotic area.

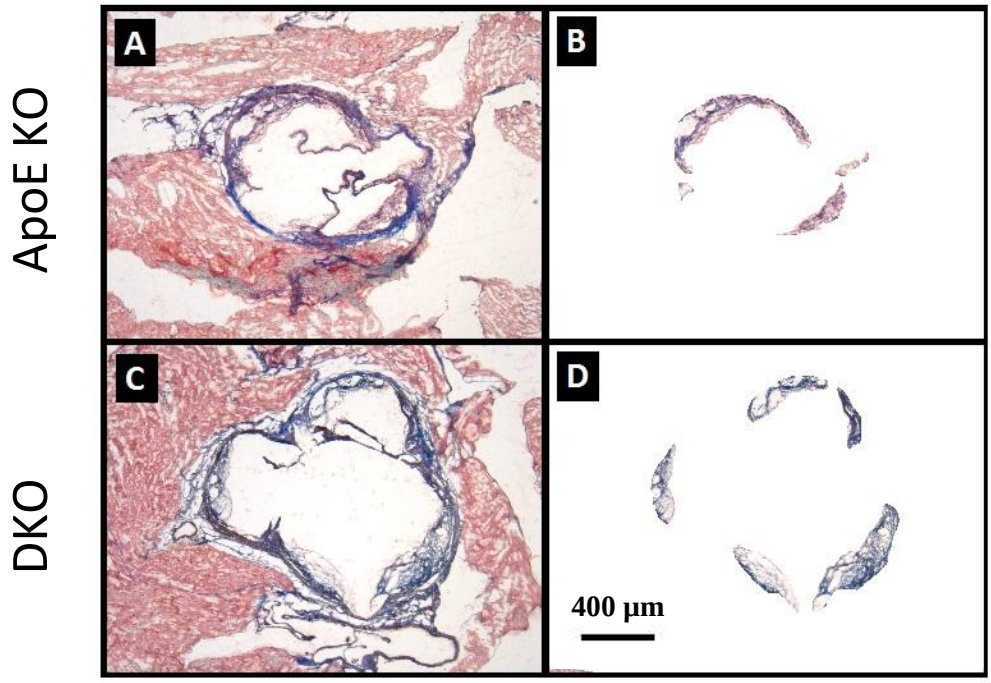

Figure 1: Trichrome Collagen Staining

(A) Trichrome collagen stained aortic root section from ApoE$^{-/-}$ mouse, full image at 50x magnification. (B) Trichrome collagen stained aortic root section from ApoE$^{-/-}$ mouse, isolated plaque image at 50x magnification used for Image J analysis. (C) Trichrome collagen stained aortic root section from ApoE$^{-/-}$/Ron$^{-/-}$ mouse, full image at 50x magnification. (D) Trichrome collagen stained aortic root section from ApoE$^{-/-}$/Ron$^{-/-}$ mouse, isolated plaque image at 50x magnification used for Image J analysis.

Collagen Area

We studied the amount of collagen deposition in the plaque because previous studies have suggested that thinning of the fibrous cap, which is composed of collagen, can contribute to rupture of the plaque, causing hemorrhaging and death[1]. It was thought that mice with Ron may show a greater deposition of collagen, thus suggesting it plays a protective role by lessening the thinning of the fibrous cap. The percentage of plaque area stained for collagen was calculated by taking the area of the collagen stain, dividing it by the total plaque area of the sample and multiplying by 100. The average percent area for both genotypes of mice is shown in Figure 2

below. The average percent collagen area for the ApoE$^{-/-}$ mice was 46.1%. The average percent collagen area for the DKO mice was 48.2%. The error bars in Figure 2 are representative of 1 standard deviation from the average of percent collagen area.

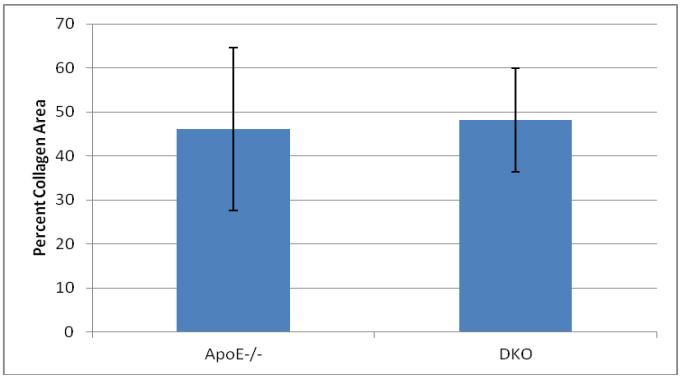

Figure 2: Average Percent Collagen Area

This figure shows the average (mean) percent of atherosclerotic plaque area stained for collagen presence using the trichrome collagen staining in the ApoE$^{-/-}$ and ApoE$^{-/-}$/Ron$^{-/-}$ (DKO) tissue samples. p = 0.78, n = 11,8. Data represent means +/-SD.

Table 1 includes the collagen area, the total area, and the percent area (collagen area/total area) for each of the ApoE$^{-/-}$ mice samples using the analyze measurement tool on the Image J software. Table 2 includes the collagen area, the total area, and the percent area for each of the double knockout mice. A t-test was used to compare the percentage of plaque area stained for collagen between the ApoE$^{-/-}$ tissue samples and the ApoE$^{-/-}$ / Ron$^{-/-}$ tissue samples and the p-value was 0.78. For the ApoE$^{-/-}$ group n=11 and for the DKO group n=8. Since no difference was found between the presence or absence of Ron in relation to collagen presence, Ron may not protect against lesion rupture by way of affecting collagen presence in the plaques.

Necrotic Area

Since Ron has been shown to promote development of M2 macrophages, those associated with apoptotic cell clearance and wound repair, it was expected that mice with the Ron receptor would have a less necrosis present in the forming lesions. A decrease in the amount of necrotic area in the plaques of mice with Ron would support the hypothesis that Ron plays a protective role in lesion progression. The necrotic area of the plaques was first analyzed using trichrome collagen staining. The necrotic area was considered to be the non-collagen stained portion of the identified plaque area, typically seen as a visible core area. The measured necrotic area and the total plaque area as measured using Image J measurements are located in Table 3 and Table 4. The percent necrotic area was calculated by dividing the necrotic area by the total plaque area and multiplied by 100, also seen in Tables 3 and 4. Table 3 is the $ApoE^{-/-}$ tissue samples and Table 4 is the DKO tissue samples.

A t-test run to compare the $ApoE^{-/-}$ and DKO percent necrotic areas and showed a p-value of 0.86. For the $ApoE^{-/-}$ group n=11 and for the DKO group n=8. Figure 3, below, displays the average percent necrotic area for the $ApoE^{-/-}$ and DKO mice groups. The average percent necrotic area for the $ApoE^{-/-}$ mice was 40.0% and the average area for the DKO mice was 38.8%. The error bars present on the figure are representative of 1 standard deviation from the average percentage of necrotic area. These calculations did not show a difference in the amount of necrosis between the two genotypes, suggesting Ron did not affect the progression of this visible necrotic core.

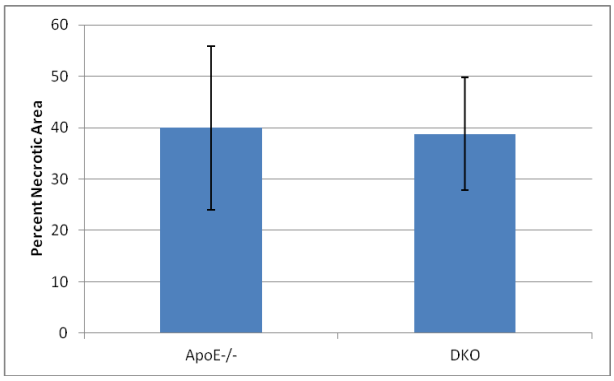

Figure 3: Average Percent Necrotic Area on Collagen Stain

This figure shows the average (mean) necrotic area in the atherosclerotic plaque measured on the trichrome collagen stain images in the ApoE$^{-/-}$ and ApoE$^{-/-}$/Ron$^{-/-}$ (DKO) tissue samples. p = 0.86, n =11,8. Data show means +/- SD.

TUNEL Assay

Next, we imaged aortic root samples from the TUNEL assay under 200x magnification by fluorescence microscopy in order to study apoptotic cell presence in the plaques as well as further study the extent of necrosis. Images were taken to view the green fluorescence protein (GFP) stain, which labels DNA strand breaks to identify the apoptotic cells. It was also used to view the DAPI stain (blue) which tags nuclei of all cells. Below, in Figure 4, you can see the GFP and DAPI stain for both an ApoE$^{-/-}$ (A, B) and double knock out (C, D) samples. The outer edge of the plaque is marked with the dashed line and the necrotic area is outlined and labeled “nec” used for the second TUNEL analysis below.

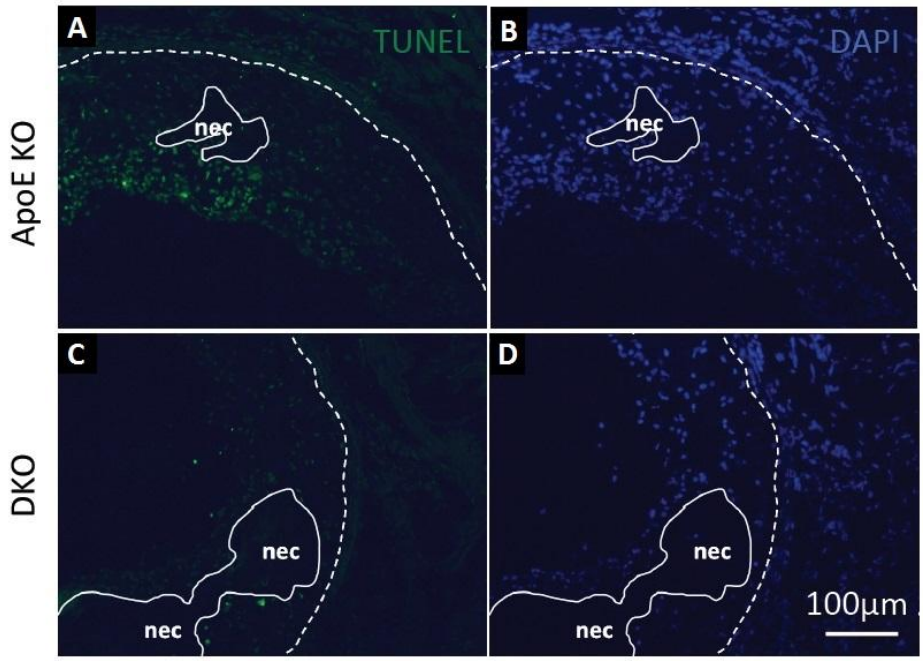

Figure 4: TUNEL Assay Images: GFP and DAPI

(A) GFP labeled aortic root section from ApoE$^{-/-}$ mouse to visualize apoptotic cells at 200x magnification. (B) DAPI labeled aortic root section from ApoE$^{-/-}$ mouse to visualize cell nuclei at 200x magnification. (C) GFP labeled aortic root section from ApoE$^{-/-}$/Ron$^{-/-}$ mouse at 200x magnification. (D) DAPI labeled aortic root section from ApoE$^{-/-}$/Ron$^{-/-}$ mouse at 200x magnification. Apoptotic cell counts within the plaque area were taken from (A) and (C) using Image J software. Total cell counts within the plaque area were taken from (B) and (D) using Image J software. Outer edge of the plaque area is marked with a dashed line and the necrotic area is outlined and labeled "nec" in all images.

TUNEL Assay Cell Counts

With the aim of seeing if the presence or absence of Ron influenced the amount of apoptosis occurring in the lesions, the quantity of cells undergoing apoptosis in the plaques were analyzed using TUNEL assay. It was first expected that there would be a larger portion of cells in the samples lacking Ron. Using Image J software, the total number of cells undergoing apoptosis (GFP) and the total number of cells (DAPI) within the plaque were counted and recorded. The percentage of cells undergoing apoptosis within the lesion was found by taking the number of apoptotic cells divided by the total number of cells and multiplying by 100. All of

these data can be found in Table 5 and Table 6. Table 5 contains the cell counts from the $ApoE^{-/-}$ tissue samples and Table 6 contains the date from the $ApoE^{-/-}/Ron^{-/-}$ tissue samples.

In 3 of the samples, 1 from the $ApoE^{-/-}$ group and 2 from the DKO group, the number of apoptotic cells counted (GFP) was above the total cell count (DAPI) by the Image J software. Since it is not possible for more than 100% of the cells present in the lesion to be undergoing apoptosis, these data were looked at with and without these samples in question. This error is thought to be an issue between the imaging of the sample and the quantitative technique of the software used for counting. In this case, two t-tests were run to analyze the data. The first was run using all the percentages calculated, including three samples where the percentage was above 100%. For this run, n=18 for the $ApoE^{-/-}$ genotype and n=19 for the DKO genotype and the p-value was 0.054.

Next, a t-test was run, eliminating the samples in question where the total percentage was greater than 100%. The data used for this t-test can be viewed in Table 7 and Table 8. For this run, n=17 for the $ApoE^{-/-}$ genotype and n=17 for the DKO genotype and the p-value was 0.017. These data show a significantly greater amount of cells present in the lesions of mice with the Ron receptor. This may suggest that Ron promotes apoptosis as a way to protect against lesion progression in atherosclerosis.

For this data set, the average percentage of apoptotic cells for both genotypes was calculated twice. The first was inclusive of the three samples in question, where the total percentage was greater than 100 and the second was the average after eliminating these 3 data points. Both averages can be seen in Figure 5 below. The error bars present on the figure are representative of 1 standard deviation from the average apoptotic cell percentage.

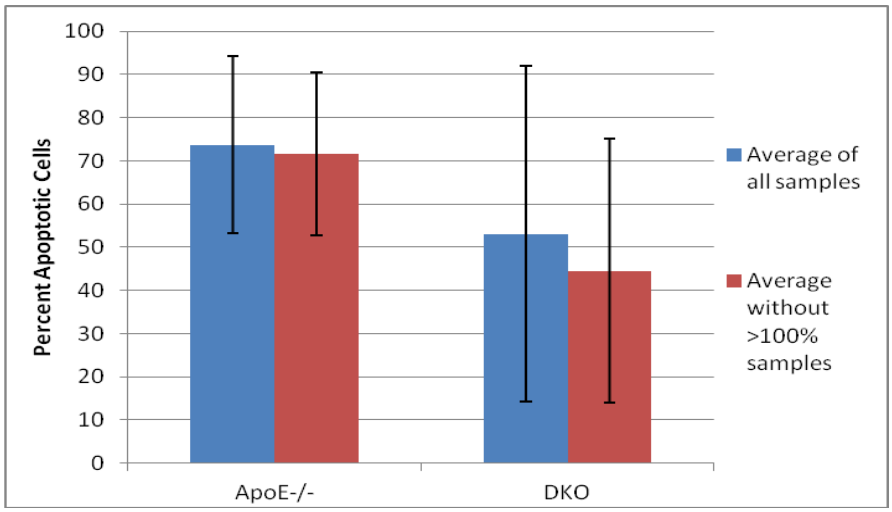

Figure 5: Percent Apoptotic Cells in Plaque Area

This figure displays the average (mean) percentage of cells undergoing apoptosis in the plaque area in ApoE$^{-/-}$ and ApoE$^{-/-}$/Ron$^{-/-}$ (DKO) tissue samples. The blue bars show the average when 3 samples in question (calculated percentage over 100%) were included in the calculation. The red bars show the average when the 3 samples in question were excluded. The error bars represent 1 standard deviation from the mean. For the blue bars, p=0.054, n=18,19. Data represent means +/-SD. For the red bars, p=0.017, n=17,17. Data shows means +/-SD.

TUNEL Assay Necrotic Core

To better understand the progression of necrosis in the atherosclerotic plaques and to try to gain a better understanding of the connection between apoptosis and necrotic area, necrotic area of the plaques were measured on the TUNEL assay images. We expected necrosis to be more advanced in tissue samples of mice lacking the Ron receptor, because is was hypothesized that Ron plays a protective role in the advancement of atherosclerotic lesions. Also, possibly identifying a connection between apoptosis and necrosis progression in the lesion may help up to better understand the way in which Ron may act in this protective role. This measuring of the necrotic core was done using the merged GFP/DAPI images for each sample. The necrotic area was considered to be the area in the plaque where there were no apoptotic cells or cell nuclei present, as can be seen outlined and labeled “nec” on the TUNEL assay images in Figure 4.

The samples were separated by genotype, $ApoE^{-/-}$ and DKO, where necrotic area and total plaque area were measure using Image J measurement analysis and recorded in Table 9 ($ApoE^{-/-}$) and Table 10 (DKO). The percentage necrotic area was calculated for each group by dividing the necrotic area by the total plaque area and multiplying by 100. The percentages are shown on Table 9 and Table 10. A t-test was run where n=18 for the $ApoE^{-/-}$ group and n=19 for the $ApoE^{-/-}/Ron^{-/-}$ group and the p-value was 0.063. The average percent necrotic area was calculated for the $ApoE^{-/-}$ and DKO aortic root samples and are show below in Figure 6. The average percent necrotic area for $ApoE^{-/-}$ tissue samples was 19.0% and the average for DKO tissue samples was 24.5%. The error bars on Figure 6 express 1 standard deviation from the average percent necrotic area.

The t-test indicated that there was no difference in the progression of necrosis in the presence or absence of the Ron receptor. However, because the p-value was less than 0.1, it suggests there may be a trend towards a greater amount of necrosis in samples from mice lacking the Ron receptor. Increasing the sample size may reveal a difference in the amount of necrosis between the genotypes. It may also be beneficial to study the amount of necrosis in younger mice with less advanced lesions, to identify if there is a difference in amount of necrosis in earlier lesions.

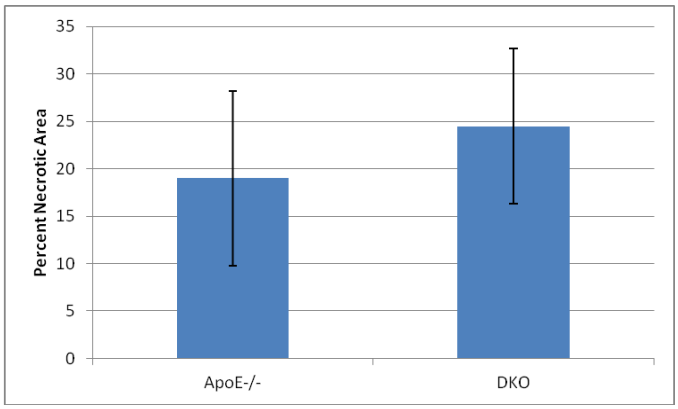

Figure 6: Percent Necrotic Area from TUNEL

This figure shows the average (mean) necrotic area in the atherosclerotic plaque measured on the TUNEL assay images in the ApoE$^{-/-}$ and ApoE$^{-/-}$/Ron$^{-/-}$ (DKO) tissue samples. $p = 0.63$, $n = 18,19$. Data represent means +/-SD.

Chapter 4 : Discussion

The purpose of this research was to take a closer look at the composition of atherosclerotic plaques in hopes of gaining a better understanding of the role the receptor tyrosine kinase Ron plays in the progression of atherosclerosis. It is known that Ron is expressed in subset of macrophages, and that it promotes the development of M2 macrophages and their function in tissue repair and apoptotic cell clearance. Since the progression of atherosclerosis is associated with an increase in M1 macrophages associated with proinflammatory processes and a decrease in M2 macrophages associated with repair and cell clearance, it is thought the activity of Ron may alter the balance of macrophage activation. In an attempt to better understand the composition of the plaques we investigated the presence of collagen, necrotic areas, and the presence of apoptotic cells in atherosclerotic plaques formed in mice predisposed to form lesions.

The first part of my studies used trichrome collagen staining of aortic root samples. Tissue samples of single knock out ($ApoE^{-/-}$) mice were compared with tissue samples of double knock out ($ApoE^{-/-}/Ron^{-/-}$) mice with respect to possible changes in percent area of the plaque that was positively stained for collagen. Unexpectedly, a t-test showed a p-value of 0.78, indicating that the amount of collagen per area between the two groups was unaffected by the absence of Ron. This suggests that Ron may not protect against lesion rupture with respect to thinning of the fibrous cap, composed of collagen, which can lead to hemorrhaging and death.

The necrotic area of $ApoE^{-/-}$ and $ApoE^{-/-}/Ron^{-/-}$ tissue samples were also compared using trichrome collagen staining and measuring the area within a plaque that appeared to form a visible core. As before, a t-test showed that there was no difference between genotypes and thus that Ron did not affect the size of the necrotic area. Upon further review, it was thought that this

method to measure a necrotic core was likely lacking in accuracy since a lack of collagen is not the single requirement for an area within a plaque to be a necrotic core area. Using the TUNEL stained samples was thought to be a more accurate way to identify necrotic areas within the plaques.

While this collagen stain was not conclusive in determining more about how Ron affects the composition of atherosclerotic plaques, it does not exclude the examination of collagen as an important characteristic to understand in the progression of the disease. Additional methods of sample staining or imaging could be beneficial for future studies of collagen deposition in atherosclerotic plaques. A technique which may help provide a better view into the collagen plaque composition is FT-IR spectroscopy. Studies have shown that this type of imaging and histology can better characterize the biochemical composition of atherosclerotic plaques. It has the potential to analyze the lipids, connective tissues, calcifications, and other cellular debris contained in the plaque[16]. Upon gaining a better view of the complicated structural components of atherosclerotic plaques, it may be possible to target more specific differences between mice that have or lack the Ron receptor gene.

Next, atherosclerotic tissue samples were analyzed by TUNEL assay to assess possible effects of Ron in apoptosis. The $ApoE^{-/-}$ single knock out group had a significantly higher percentage of apoptotic cells present in the plaque area than the DKO group. In three samples the calculated apoptotic cell percentage was greater than 100%. Since it is not possible to have greater than 100% of cells undergoing apoptosis, this was thought to be an issue with the staining or imaging of these samples, which then caused difficulty for the software when trying to analyze and count the apoptotic cells and the cell nuclei. The data was included for both the complete data set in which case the three samples in question were kept in the calculations as well as the calculations when these three samples were excluded from the calculation. A t-test was run for both of these data sets. When the three samples in question were included the p-value was 0.054.

With these three samples excluded, the p-value was 0.017, which is considered to be a statistically significant difference in the percentage of cells undergoing apoptosis between the genotypes.

The finding that the group that has the Ron receptor gene has a greater percentage of apoptotic cells in the total plaque area must be looked at alongside other data collected for the samples. By itself, it may seem intuitive to think more apoptotic cell presence must indicate a further progression of the plaque. However, this is not necessarily the case. In the progression of atherosclerotic lesions, the cells in the plaque must die, but often remains of cellular debris remain in the necrotic core, which is indicative of a more advanced lesion. In the case where the cells in the plaque undergo apoptosis and cell clearance, there is less opportunity for necrosis to take place. In this case, one would expect to see more apoptotic cells in a less advanced lesion than in a more advanced lesion, and would be supported if it was also noted that the lesion thought to be more advanced has a greater necrotic area, or total plaque area. To better understand this, it is best to connect these conclusions to other images analyzed in the research.

The final portion of my research used the TUNEL assay images to measure the amount of necrosis in the atherosclerotic lesions. The necrotic areas were identified as areas lacking cell nuclei and apoptotic cells in merged GFP/DAPI stained images. The average percent necrotic area of the plaque appeared to be greater in the samples lacking the Ron receptor, than in $ApoE^{-/-}$ samples. However, comparing the necrotic areas between the sample groups using a t-test showed that there was no difference. Although no difference was found, because the p-value (0.063) was below 0.1, the results suggest a possible trend in the data. This may suggest a trend towards greater necrotic area in mice lacking the Ron receptor. It is thought that a significant difference may be seen if the sample size were to be increased. This is partially due to the large standard deviation from the average percent necrotic area observed in both $ApoE^{-/-}$ and $ApoE^{-/-}/Ron^{-/-}$ tissue samples. Taking this data into account with the previous data about the amount of

apoptotic cells present in the plaque areas, it is thought that these results may provide support for the hypothesis that Ron plays a protective role in the progression of atherosclerosis.

To conclude, atherosclerosis is one chronic inflammatory condition that is a very prominent issue in the medical field today. The role of inflammation in atherosclerosis progression, as well as other health problems such as hypertension and obesity, is still a very active field of study. The hope is to advance our understanding of the complex nature of these diseases, such that in the future we will be able to provide better therapies and solutions to the issues facing those suffering today. By gaining a better understanding of how the composition of the plaques in atherosclerosis progresses with respect to the Ron receptor tyrosine kinase, we will hopefully be able to find better, more efficient ways to diagnose and treat these conditions.

Appendix

Complete Data Tables

Table 1: Trichrome Collagen Stain: ApoE$^{-/-}$ Collagen Area

Sample	Collagen Area (in.^{2})	Total Area (in.^{2})	Percent Area (%)
8/28/12 H8	4.036	7.177	56.2
9/17/12 H1	2.278	4.800	47.5
9/17/12 H13	1.431	6.480	22.1
9/26/12 H1	1.484	6.995	21.2
9/26/12 H2	4.710	11.551	40.8
2/19/13 H2	2.165	3.082	70.2
2/19/13 H3	4.262	6.080	70.1
2/19/13 H5	4.734	6.895	68.7
8/28/12 H7	1.291	4.699	27.5
8/28/12 H10	3.397	7.449	45.6
8/28/12 H11	0.913	2.459	37.1
Average	**2.791**	**6.152**	**46.1**

The table below displays data collected from aortic root atherosclerotic plaques of ApoE$^{-/-}$ mice stained with trichrome collagen stain imaged at 50x magnification. Collagen area and total plaque area were measured through an Image J threshold measurement analysis process. The process (described fully in methods) measured area of plaque positively stained for collagen followed by total area of isolated plaque in the image. Figure 1 (B) shows an example of the isolated plaque image used for analysis. Percent area was calculated for each of the 11 samples [(collagen area/total area)*100].

Table 2: Trichrome Collagen Stain: ApoE$^{-/-}$/Ron$^{-/-}$ Collagen Area

Sample	Collagen Area (in^2)	Total Area (in.^{2})	Percent Area (%)
8/28/12 H 16	4.872	9.342	52.2
9/26/12 H5	4.843	11.140	43.5
9/26/12 H6	1.359	3.103	43.8
9/26/12 H7	1.560	2.943	53.0
9/26/12 H9	2.653	8.778	30.2
2/19/13 H7	2.244	4.028	55.7
2/19/13 H9	3.075	4.495	68.4
8/28/12 H12	1.278	3.300	38.7
Average	**2.736**	**5.891**	**48.2**

The table below displays data collected from aortic root atherosclerotic plaques of ApoE$^{-/-}$/Ron$^{-/-}$ mice stained with trichrome collagen stain imaged at 50x magnification. Collagen area and total plaque area were measured through an Image J threshold measurement analysis process. The process (described fully in methods) measured area of plaque positively stained for collagen followed by total area of isolated plaque in the image. Figure 1 (D) shows an example of the isolated plaque image used for analysis. Percent area was calculated for each of the 8 samples [(collagen area/total area)*100].

Table 3: Trichrome Collagen Stain: ApoE$^{-/-}$ Necrotic Area

Sample	Necrotic Area (in.^{2})	Total Area (in.^{2})	Percent Area (%)
8/28/12 H8	2.208	7.177	30.8
9/17/12 H1	1.679	4.800	35.0
9/17/12 H13	4.008	6.480	61.9
9/26/12 H1	4.090	6.995	58.5
9/26/12 H2	5.242	11.551	45.4
2/19/13 H2	0.636	3.082	20.6
2/19/13 H3	1.262	6.080	20.8
2/19/13 H5	1.367	6.895	19.8
8/28/12 H7	2.439	4.699	51.9
8/28/12 H10	2.828	7.449	38.0
8/28/12 H11	1.402	2.459	57.0
Average	**2.469**	**6.152**	**40.0**

This table displays data collected from aortic root atherosclerotic plaques of ApoE$^{-/-}$ mice stained with trichrome collagen stain imaged at 50x magnification. Necrotic area and total plaque area were measured through an Image J measurement analysis process. The process (described fully in methods) measured the area of the outlined necrotic area. The total plaque area of the samples was measure previously as listed in the collagen area data tables and was again used for this analysis. Figure 1 (B) shows an example of the isolated plaque image used for analysis. Percent area was calculated for each of the 11 samples [(necrotic area/total area)*100].

Table 4: Trichrome Collagen Stain: ApoE$^{-/-}$/Ron$^{-/-}$ Necrotic Area

Sample	Necrotic Area (in.^{2})	Total Area (in.^{2})	Percent Area (%)
8/28/12 H 16	3.150	9.342	33.7
9/26/12 H5	4.709	11.140	42.3
9/26/12 H6	1.430	3.103	46.1
9/26/12 H7	1.095	2.943	37.2
9/26/12 H9	4.947	8.778	56.4
2/19/13 H7	1.114	4.028	27.7
2/19/13 H9	1.000	4.495	22.2
8/28/12 H12	1.475	3.300	44.7
Average	**2.365**	**5.891**	**38.8**

This table displays data collected from aortic root atherosclerotic plaques of ApoE$^{-/-}$/Ron$^{-/-}$ mice stained with trichrome collagen stain imaged at 50x magnification. Necrotic area and total plaque area were measured through an Image J measurement analysis process. The process (described fully in methods) measured the area of the outlined necrotic area. The total plaque area of the samples was measure previously as listed in the collagen area data tables and was again used for this analysis. Figure 1 (D) shows an example of the isolated plaque image used for analysis. Percent area was calculated for each of the 8 samples [(necrotic area/total area)*100].

Table 5: TUNEL Cell Counts: ApoE$^{-/-}$

Sample	Apoptotic Cells (GFP)	Total Cells (DAPI)	Percentage (%)
3/26/2012 H1 - 1	76	84	90.5
3/26/2012 H1 - 2	113	200	56.5
3/26/2012 H1 - 3	89	154	57.8
8/28/12 H8 - 1	154	264	58.3
8/28/12 H8 - 2	310	339	91.4
8/28/12 H8 - 3	65	168	38.7
8/28/12 H10 - 1	163	166	98.2
8/28/12 H10 - 2	54	117	46.2
8/28/12 H10 - 3	99	100	99.0
9/17/12 H1 - 1	**209**	**189**	**110.6**
9/17/12 H1 - 2	182	222	82.0
9/17/12 H1 - 3	112	160	70.0
9/26/12 H1 - 1	203	317	64.0
9/26/12 H1 - 2	121	172	70.3
9/26/12 H1 - 3	38	43	88.4
9/26/12 H2 - 1	150	256	58.6
9/26/12 H2 - 2	119	133	89.5
9/26/12 H2 - 3	177	314	56.4
Average	**135.22**	**188.78**	**73.7**

This table below displays TUNEL assay data collected from aortic root atherosclerotic plaques of ApoE$^{-/-}$ mice. The number of apoptotic cells (labeled with GFP) in the atherosclerotic plaque area were quantified using Image J software. The total number of cells present in the plaque area (nuclei labeled with DAPI) was also quantified using Image J. The percentage of cells undergoing apoptosis was calculated for each of the 18 samples [(apoptotic cells/total cells)*100]. The 18 samples were 18 different plaque regions imaged on 6 different aortic root samples at 200x magnification. The 9/17/12 H1 – 1 sample showed a calculated percentage over 100%, which is not possible as a percentage of total cells in the plaque, and was thus excluded from calculation as shown in Table 7.

Table 6: TUNEL Cell Counts: ApoE$^{-/-}$/Ron$^{-/-}$

Sample	Apoptotic Cells (GFP)	Total Cells (DAPI)	Percentage (%)
9/26/13 H5 - 1	155	203	76.4
9/26/13 H5 - 2	**333**	**295**	**112.9**
9/26/13 H5 - 3	124	182	68.1
3/26/12 H6 - 1	82	218	37.6
3/26/12 H6 - 2	50	302	16.6
3/26/12 H6 - 3	**88**	**63**	**139.7**
3/26/12 H7 - 1	57	140	40.7
3/26/12 H7 - 2	62	85	72.9
3/26/12 H7 - 3	15	61	24.6
3/26/12 H8 - 1	16	108	14.8
3/26/12 H8 - 2	30	109	27.5
3/26/12 H8 - 3	18	169	10.7
8/28/12 H16 - 1	104	109	95.4
8/28/12 H16 - 2	33	150	22.0
8/28/12 H16 - 3	12	186	6.5
3/26/12 H9 - 1	101	139	72.7
3/26/12 H9 - 2	236	242	97.5
3/26/12 H9 - 3	52	299	17.4
3/26/12 H9 - 4	68	124	54.8
Average	**86.11**	**167.58**	**53.1**

This table below displays TUNEL assay data collected from aortic root atherosclerotic plaques of ApoE$^{-/-}$/Ron$^{-/-}$ mice. The number of apoptotic cells (labeled with GFP) in the atherosclerotic plaque area were quantified using Image J software. The total number of cells present in the plaque area (nuclei labeled with DAPI) was also quantified using Image J. The percentage of cells undergoing apoptosis was calculated for each of the 19 samples [(apoptotic cells/total cells)*100]. The 19 samples were 19 different plaque regions imaged on 6 different aortic root samples at 200x magnification. The 9/26/12 H5 – 2 and the 3/26/12 H6 -3 samples showed a calculated percentage over 100%, which is not possible as a percentage of total cells in the plaque undergoing apoptosis, and was thus excluded from calculation as shown in Table 8.

Table 7: TUNEL Cell Counts (>100% removed): ApoE$^{-/-}$

Sample	Apoptotic Cells (GFP)	Total Cells (DAPI)	Percentage (%)
3/26/2012 H1 – 1	76	84	90.5
3/26/2012 H1 – 2	113	200	56.5
3/26/2012 H1 – 3	89	154	57.8
8/28/12 H8 – 1	154	264	58.3
8/28/12 H8 – 2	310	339	91.4
8/28/12 H8 – 3	65	168	38.7
8/28/12 H10 – 1	163	166	98.2
8/28/12 H10 – 2	54	117	46.2
8/28/12 H10 – 3	99	100	99.0
9/17/12 H1 – 2	182	222	82.0
9/17/12 H1 – 3	112	160	70.0
9/26/12 H1 – 1	203	317	64.0
9/26/12 H1 – 2	121	172	70.3
9/26/12 H1 – 3	38	43	88.4
9/26/12 H2 – 1	150	256	58.6
9/26/12 H2 – 2	119	133	89.5
9/26/12 H2 – 3	177	314	56.4
Average	**130.88**	**188.76**	**71.5**

The table below displays TUNEL assay data collected from aortic root atherosclerotic plaques of ApoE$^{-/-}$ mice. The number of apoptotic cells (labeled with GFP) in the atherosclerotic plaque area were quantified using Image J software. The total number of cells present in the plaque area (nuclei labeled with DAPI) was also quantified using Image J. The percentage of cells undergoing apoptosis was calculated for each of the 17 samples [(apoptotic cells/total cells)*100]. The 1 samples were 17 different plaque regions imaged on 6 different aortic root samples at 200x magnification. A single sample in question, that had a calculated percentage greater than 100%, was excluded from the table and calculations.

Table 8: TUNEL Cell Counts (>100% removed): ApoE$^{-/-}$/Ron$^{-/-}$

Sample	Apoptotic Cells (GFP)	Total Cells (DAPI)	Percentage (%)
9/26/13 H5 - 1	155	203	76.4
9/26/13 H5 - 3	124	182	68.1
3/26/12 H6 - 1	82	218	37.6
3/26/12 H6 - 2	50	302	16.6
3/26/12 H7 - 1	57	140	40.7
3/26/12 H7 - 2	62	85	72.9
3/26/12 H7 - 3	15	61	24.6
3/26/12 H8 - 1	16	108	14.8
3/26/12 H8 - 2	30	109	27.5
3/26/12 H8 - 3	18	169	10.7
8/28/12 H16 - 1	104	109	95.4
8/28/12 H16 - 2	33	150	22.0
8/28/12 H16 - 3	12	186	6.5
3/26/12 H9 - 1	101	139	72.7
3/26/12 H9 - 2	236	242	97.5
3/26/12 H9 - 3	52	299	17.4
3/26/12 H9 - 4	68	124	54.8
Average	**71.47**	**166.24**	**44.5**

This table displays TUNEL assay data collected from aortic root atherosclerotic plaques of ApoE$^{-/-}$/Ron$^{-/-}$ mice. The number of apoptotic cells (labeled with GFP) in the atherosclerotic plaque area were quantified using Image J software. The total number of cells present in the plaque area (nuclei labeled with DAPI) was also quantified using Image J. The percentage of cells undergoing apoptosis was calculated for each of the 17 samples [(apoptotic cells/total cells)*100]. The 17 samples were 17 different plaque regions imaged on 6 different aortic root samples at 200x magnification. Two samples in question were excluded from the table and further calculations because the calculated percentage of apoptotic cells was greater than 100%, which is not possible.

Table 9: TUNEL Necrotic Area: ApoE$^{-/-}$

Sample	Necrotic Area (pixels)	Total Area (pixels)	Percentage (%)
3/26/2012 H1 - 1	145023	341483	42.5
3/26/2012 H1 - 2	96292	488096	19.7
3/26/2012 H1 - 3	89377	398692	22.4
8/28/12 H8 - 1	79543	646198	12.3
8/28/12 H8 - 2	77240	703641	11.0
8/28/12 H8 - 3	87587	551718	15.9
8/28/12 H10 - 1	53198	452725	11.8
8/28/12 H10 - 2	63970	307493	20.8
8/28/12 H10 - 3	45822	281517	16.3
9/17/12 H1 - 1	234183	852278	27.5
9/17/12 H1 - 2	150556	586637	25.7
9/17/12 H1 - 3	145754	506193	28.8
9/26/12 H1 - 1	76844	663974	11.6
9/26/12 H1 - 2	80805	507329	15.9
9/26/12 H1 - 3	103537	352996	29.3
9/26/12 H2 - 1	23809	475803	5.0
9/26/12 H2 - 2	28539	342200	8.3
9/26/12 H2 - 3	151563	882820	17.2
Average	**96313.44**	**518988.50**	**19.0**

This table below displays TUNEL assay image data collected from aortic root atherosclerotic plaques of ApoE$^{-/-}$ mice imaged at 200x magnification as a 1360X1040 pixels image. Necrotic area and total plaque area were measured in number of pixels. This process (described fully in methods) measured the area of the outlined necrotic area followed by the outlined total plaque area on merged GFP/DAPI images. Figure 4 (A) (B) shows examples of the GFP/DAPI images used for analysis with the outlined necrotic area. Percent area was calculated for each of the 18 samples [(necrotic area/total area)*100]. The 18 samples were 18 different plaque regions of 6 different tissue samples.

Table 10: TUNEL Necrotic Area: ApoE$^{-/-}$/Ron$^{-/-}$

Sample	Necrotic Area (pixels)	Total Area (pixels)	Percentage (%)
9/26/13 H5 - 1	111535	553968	20.1
9/26/13 H5 - 2	59009	455106	13.0
9/26/13 H5 - 3	140071	548064	25.6
3/26/12 H6 - 1	97274	521350	18.7
3/26/12 H6 - 2	185298	734399	25.2
3/26/12 H6 - 3	188429	466635	40.4
3/26/12 H7 - 1	209855	723914	29.0
3/26/12 H7 - 2	265497	717604	37.0
3/26/12 H7 - 3	105304	320523	32.9
3/26/12 H8 - 1	70765	346132	20.4
3/26/12 H8 - 2	209311	563190	37.2
3/26/12 H8 - 3	127266	518524	24.5
8/28/12 H16 - 1	161101	521595	30.9
8/28/12 H16 - 2	85053	405810	21.0
8/28/12 H16 - 3	120608	513431	23.5
3/26/12 H9 - 1	52672	368591	14.3
3/26/12 H9 - 2	97752	630081	15.5
3/26/12 H9 - 3	115315	755156	15.3
3/26/12 H9 - 4	85325	411549	20.7
Average	**130917.89**	**530295.89**	**24.5**

This table shows TUNEL assay image data collected from aortic root atherosclerotic plaques of ApoE$^{-/-}$/Ron$^{-/-}$ mice imaged at 200x magnification as a 1360X1040 pixels image. Necrotic area and total plaque area were measured in number of pixels. This process (described fully in methods) measured the area of the outlined necrotic area followed by the outlined total plaque area on merged GFP/DAPI images. Figure 4 (C) (D) shows examples of the GFP/DAPI images used for analysis with the outlined necrotic area. Percent area was calculated for each of the 19 samples [(necrotic area/total area)*100]. The 19 samples were 19 different plaque regions of 6 different tissue samples.

BIBLIOGRAPHY

1. Nakano, M., Stephen, J., Kramer, M. C.A., Ladich, E. R., Kolodgie, F. D., & Virmani, R. (2013). Insights into the natural history of atherosclerosis progression. *Atherosclerosis: Clinical Perspectives Through Imaging* (pp. 3-12).
2. Hansson, G. K., & Hermansson, A. (2011). The immune system in atherosclerosis. *Nature Immunology*, *12*, 204-212.
3. Libby, P., Ridker, P. M., & Maseri, A. (2002). Inflammation and atherosclerosis. *Circulation: Journal of the American Heart Association*, *105*, 1135-1143.
4. Stewart-Phillips, J. L., & Lough, J. (1991). Pathology of atherosclerosis in cholesterol-fed, susceptible mice. *Atherosclerosis*, *90*, 211-218.
5. Moore, K. J., & Tabas, I. (2011). Macrophages in the pathogenesis of atherosclerosis. *Cell*, *145*, 341-355.
6. Odegaard, J. I., & Chawla, A. (2011). Alternative macrophage activation and metabolism. *The Annual Review of Pathology: Mechanisms of Disease*, *27*, 275-297.
7. von der Thusen, J., van Vlijmen, B. J.M., Hoeben, R. C., Kockx, M. M., Havekes, L.M., van Berkel, T. J.C., & Biessen, E. A.L. (2002). Induction of atherosclerotic plaque rupture in apolipoprotein E-/- mice after adenovirus-mediated transfer of p53. *Circulation: Journal of the American Heart Association*, *105*, 2064-2070.
8. Thorp, E., Cui, D., Schrijvers, D. M., Kuriakose, G., & Tabas, I. (2008). Mertk receptor mutation reduces efferocytosis efficiency and promotes apoptotic cell accumulation and plaque necrosis in atherosclerosis lesions of Apoe-/- mice. *Journal of the American Heart Association*, *8*, 1421-1428.

9. Linton, M. F., & Fazio, S. (2003). Macrophages, inflammation and atherosclerosis. *International Journal of Obesity*, *27*, S35-S40.

10. Liu, J., Thewke, D. P., Su, Y. R., Linton, M. F., Fazio, S., & Sinensky, M. S. (2005). Reduced macrophage apoptosis is associated with accelerated atherosclerosis in low-density lipoprotein receptor-null mice. *Atherosclerosis, Thrombosis, and Vascular Biology: Journal of the American Heart Association*, *25*, 174-179.

11. Robinson, D. R., Wu, Y.-M., & Lin, S.-F. (2000). The protein tyrosine kinase family of the human genome. *Oncogene*, *19*, 5548-5557.

12. Guadino, G., Follenzi, A., Naldini, L., Collesi, C., Santoro, M., Gallo, K. A., . . . Comogilio, P. M. (1994). Ron is a heterodimeric tyrosine kinase receptor activated by the HGF homologue MSP. *The EMBO Journal*, *13*, 3524-3532.

13. Wetzel, D. L., Post, G. R., & Lodder, R. A. (2005). Synchrotron infrared microspectroscopic analysis of collagens I, III, and elastin on the shoulders of human thin-cap fibroatheromas. *Vibrational Spectroscopy*, 38, 1-7.

14. Belbachir, K., Noreen, R., Gouspillou, G., & Petibois, C. (2009). Collagen types analysis and differentiation by FTIR spectroscopy. *Analytical and Bioanalytical Chemistry*, *395*, 829-837.

15. Wrobel, T. P., Mateuszuk, L., Chlopicki, S., Malek, K., & Baranska, M. (2011). Imaging of lipids in atherosclerotic lesion in aorta from ApoE/LDLR-/- mice by FT-IR spectroscopy and hierarchical cluster analysis. *The Royal Society of Chemistry*, *136*, 5247-5255.

16. Li, C., Ebenstein, D., Xu, C., Chapman, J., Saloner, D., Rapp, J., & Pruitt, L. (2003). Biochemical characterization of atherosclerotic plaque constituents using FTIR spectroscopy and histology. *Wiley Periodicals*, 64A, 197-206.

17. Walker, J. A., & Quirkle, P. (2001). Viewing apoptosis through a 'TUNEL'. *Journal of Pathology*, *195*, 275-276.

18. Aigner, T. (2002). Apoptosis, necrosis, or whatever: how to find out what really happens? *Journal of Pathology*, *198*, 1-4.

19. Khallou-Lashet, J., Varthaman, A., Fornasa, G., Compain, C., Gaston, A.-T., Clement, M., . . . Nicoletti, A. (2010). Macrophage plasticity in experimental atherosclerosis. *PLOS One*, *5*, 1-10.

20. Iwama, A., Yamaguchi, N., & Suda, T. (1996). STK/RON receptor tyrosine kinase mediates both apoptotic and growth signals via multifunctional docking site conserved among the HGF factor family. *The EMBO Journal*, *15*, 5866-5875.

21. Pourcet, B., & Pineda-Torra, I. (2013). Transcriptional regulation of macrophage arginase 1 expression and its role in atherosclerosis. *Trends in Cardiovascular Medicine*, *23*, 143-152.

22. Sharda, D. R., Yu, S., Ray, M., Squadrito, M. L., De Palma, M., Wynn, T. A., . . . Hankey, P. A. (2011). Regulation of macrophage arginase expression and tumor growth by the ron receptor tyrosine kinase. *Journal of Immunology*, *187*, 2181-2192.

23. Wang, M.-H., Zhou, Y.-Q., & Chen, Y.-Q. (2002). Macrophage-stimulating protein and RON receptor tyrosine kinase: Potential regulators of macrophage inflammatory activities. *Journal of Immunology*, 56, 545-553.

24. Wang, X., & Hankey, P. (2013). The ron receptor tyrosine kinase: A key regulator of inflammation and cancer progression. *Critical Review of Immunology*, *33*, 549-574.

25. Fan, J., Watanabe, T. (2003). Inflammatory reactions in the pathogenesis of atherosclerosis. *Journal of Atherosclerosis and Thrombosis, 10*, 63-71.

26. Farb, A., Burke, A.P., Tang, A.L., Liang, T.Y., Mannan, P., Smialek, J., Virmani, R. (1996). Coronary plaque erosion without rupture into a lipid core. A frequent cause of coronary thrombosis in sudden coronary death. *Circulation, 93*, 1354-1363.

27. Gijsen, F.J., Wentzel, J.J., Thury, A., Mastik, F., Schaar J.A., Schuurbiers, J.C., Slager C.J., van der Giessen, W.J., de Feyter, P.J., van der Steen, A.F., Serruys, P.W. (2008). Strain distribution over plaques in human coronary arteries relates to sheer stress. *American Journal of Physiology Heart and Circulation Physiology, 295*, H1608-H1614.

28. Kolodgie, F.D., Burke, A.P, Farb, A., Gold, H.K., Yuan, J., Narula, J., Finn, A.V., Virmani, R. (2001). The thin-cap fibroatheroma: a type of vulnerable plaque: the major precursor lesion to acute coronary syndromes, *Current Opinion in Cardiology, 16*,285-292.

29. Johnson, J.L., Newby, A.C. (2009). Macrophage heterogeneity in atherosclerotic plaques, *Current Opinions in Lipidology, 20*, 370-378.

ACADEMIC VITA

Staci Henry

School Address:
901L W. Aaron Dr.
State College, PA 16803

slh5412@psu.edu
Mobile: (717) 808-9138

Permanent Address:
2664 Rosebay Dr.
York, PA 17408

EDUCATION

Pennsylvania State University, Schreyer Honors College – University Park, PA
B.S. in Biology, General Biology Option
Honors in Biology
Expected May 2014

Hempfield High School – Landisville, PA
Fall 2006 – Spring 2010

HONORS AND AWARDS

Academic Excellence Scholarship, Schreyer Honors College, Fall 2009 – Spring 2014
Doris N. McKinstry Scholarship, Eberly College of Science, Fall 2013 – Spring 2014

LEADERSHIP AND ACTIVITIES

Rainbow Roundtable, LGBTA Organization at Penn State
Active member, Fall 2010 – Fall 2011
– participated in club events and planning
Treasurer, Spring 2012 – Fall 2012
– maintained financial records, transactions, and organized all fundraisers
President, Spring 2013 through Fall 2013
– maintained relations with university clubs and public, managed schedule and aided with events

Alpha Epsilon Delta Pennsylvania Beta Chapter (Pre-professional Health Honor Society)
General member, Fall 2010 to Spring 2012
– participated in blood drive volunteering and other group activities including THON

Penn State Pre-Physician Assistant Club
General member, Spring 2012 to present
– participate in group activities and events

PRESENTATIONS

Role of Ron Receptor Tyrosine Kinase in Atherosclerotic Plaque Composition
Penn State Hazleton Undergraduate Research Fair ǁ April 9, 2014